HHS Public Access

Author manuscript

IEEE Trans Biomed Eng. Author manuscript; available in PMC 2024 July 10.

Published in final edited form as:

IEEE Trans Biomed Eng. 2018 February ; 65(2): 431–439. doi:10.1109/TBME.2017.2773463.

A three–dimensional (3D) arrayed microfluidic blood–brain barrier model with integrated electrical sensor array

Sehoon Jeong [Student Member, IEEE],
Department of Biomedical Engineering, Texas A&M University, College Station, TX 77843, USA

Sunja Kim,
Department of Veterinary Integrative Biosciences, Texas A&M University, College Station, TX 77843, USA

John Buonocore,
Department of Electrical and Computer Engineering, Texas A&M University, College Station, TX 77843, USA

Jaewon Park,
Department of Electrical and Electronic Engineering, Southern University of Science and Technology, Shenzhen 518055, China

C. Jane Welsh,
Department of Veterinary Integrative Biosciences, Texas A&M University, College Station, TX 77843, USA

Jianrong Li,
Department of Veterinary Integrative Biosciences, Texas A&M University, College Station, TX 77843, USA

Arum Han* **[Senior Member, IEEE]**
Department of Biomedical Engineering, Texas A&M University, College Station, TX 77843, USA

Department of Electrical and Computer Engineering, Texas A&M University, College Station, TX 77843, USA

Abstract

Objective: The blood–brain barrier (BBB) poses a unique challenge to the development of therapeutics against neurological disorders due to its impermeability to most chemical compounds. Most *in vitro* BBB models have limitations in mimicking *in vivo* conditions. Here we show a co-culture microfluidic BBB-on-a-chip that provides interactions between neurovascular endothelial cells and neuronal cells across a porous polycarbonate membrane, which better mimics the *in vivo* conditions, as well as *in vivo*-level shear stress.

Methods: A 4 × 4 intersecting microchannel array forms 16 BBB sites on a chip, with a multi-electrode array integrated to measure the trans–endothelial electrical resistance (TEER) from

*correspondence: arum.han@ece.tamu.edu.

all 16 different sites, which allows label-free real-time analysis of the barrier function. Primary mouse endothelial cells and primary astrocytes were co-cultured in the chip while applying *in vivo* level shear stress. The chip allows the barrier function to be analyzed using TEER measurement, dextran permeability, as well as immunostaining.

Results: Co-culture between astrocytes and endothelial cells, as well as *in vivo* level shear stress applied, led to the formation of tighter junctions and significantly lower barrier permeability. Moreover, drug testing with histamine showed increased permeability when using only endothelial cells compared to almost no change when using co-culture.

Conclusion: Results show that the developed BBB chip more closely mimics the *in vivo* BBB environment.

Significance: The developed multi-site BBB chip is expected to be used for screening drug candidates and their toxicity by more accurately predicting the BBB permeability of drug candidates during preclinical stages.

Index Terms—

Organ–on–a-chip; Microfluidic blood–brain barrier (BBB) on a chip; Electrical impedance sensor array; Microphysiological systems; Co-culture tissue chip

I. Introduction

IN *vitro* organ–on–a–chips are being developed to mimic the *in vivo* physiological conditions more accurately by creating three-dimensional (3D) multi–cellular tissue structures integrated with microfluidic systems. Significant efforts have been made in developing systems that can better represent structural and functional units of organs, with the purpose of facilitating new *in vitro* testing approaches to enable cost-effective and more accurate predictions of drug efficacy and toxicity [1]. In the case of new drug developments for diseases in the central nervous system (CNS), only 7% of the drugs in clinical developments have reached market place despite increased investment in this area and increasing number of patients suffering from various brain diseases [2]. One of the major reasons for the low success rate of CNS drug development is the existence of the blood–brain barrier (BBB), a highly selective barrier that protects the brain from most pathogens and potentially toxic chemical compounds while allowing the passage of molecules that are crucial to proper neural functions. While this unique barrier structure is essential for protecting CNS from potentially harmful chemicals and maintaining a stable brain environment [3], successful drug delivery through the BBB has become a major challenge for drug development against an abroad range of neurological disorders, from acute brain infection to chronic neurodegenerative diseases [4]. Thus, being able to conduct *in vitro* testing against BBB, which can be used to understand the barrier functions better and to develop new drugs against neurological diseases, is critically needed.

Conventional *in vitro* culture methods for BBB studies utilize transwell inserts that simply allow endothelial cells to be grown on a porous membrane in the upper chamber that is immersed in the growth media chamber as a vertical diffusion system, and thus partially mimicking the BBB and their environment [5, 6]. Although cells grown in such transwell

systems do show some levels of barrier functions, the functions are still quite different from those seen *in vivo* and fail to generate tissue–level functionalities, as they typically lack shear stress during culture. Physiological shear stress plays a key role in promoting neurovascular endothelial cell differentiation and BBB functions in terms of expression, localization, and association of tight junction proteins [7–9]. In addition, even though transwell platforms allow co-culture of endothelial cells with other BBB cell types such as astrocytes and pericytes in the lower chamber, this results in large distance between the two cell types (from the top of the membrane to the bottom of the culture well), which is quite different from the *in vivo* environment where those two cell types are located close together within tens of micrometers. Alternatively, astrocytes and pericytes can be cultured on the backside of the porous membrane of a transwell insert, but achieving cell uniformity and batch-to-batch variations are extremely challenging during cell seeding on the backside of the transwell inserts. Accordingly, the endothelial cells often lack the necessary factors needed for the proper development and maintenance of BBB properties. As a result, the measured trans–endothelial electrical resistance (TEER) level, an indicator of barrier integrity, are typically lower and also often show irregular patterns due to cell adhesion or cell uniformity issues [6].

To overcome some of these limitations, *in vitro* BBB models that have flow chambers or capillary–like 3D configurations, where applying shear stress to endothelial cell culture or culturing both endothelial cells and astrocytes on the inside and outside of hollow fibers for enabling co-culture conditions are possible, have been developed [10, 11]. Nevertheless, there still remains a large gap in physiological functions that can be achieved by these *in vitro* systems compared to *in vivo* systems. This is in part due to the significantly lower shear stress applied compared to *in vivo* conditions because of their relatively large inner chamber and lack of primary cells used in such systems, to name a few [6, 12]. In addition, these systems are not amenable for high-throughput screening applications, as each setup is complicated and takes a significant amount of cost and effort to setup.

In recent years, several microfluidic BBB models that better mimic *in vivo* BBB functions have been developed. There are largely two different configurations of microfluidic BBB–on–a–chip systems, the planar types and the vertical types. The planar microfluidic BBB models typically utilize arrays of micropillars or microchannels as a boundary between the blood and brain side of chambers. The gaps between these microstructures are small enough to trap cells on either side and thus allow endothelial cells and astrocytes to be cultured on each side of the microstructures, functioning in a similar manner as a vertically placed porous membrane [13]. However, there are several limitations. The channel length of the interface connecting both the luminal and the abluminal sides was 50 μm, which is much longer than the distance between endothelial cells and astrocytes in *in vivo* (≤1 μm), and even compared to those in transwell inserts (10 – 20 μm). On the other hand, the vertical microfluidic BBB models typically utilize the same type of porous membranes used in transwell culture as a boundary between the blood and brain side of chambers. This porous membrane is sandwiched between two microfluidic structures, one side serving as the blood vessel side and the other side serving as the brain tissue side [14]. However, initially no shear stress was applied to the culture and the culture time was limited to 2–3 days because of the inaccessibility to the neuronal side of the system. A more advanced model integrated

the aforementioned structural advantages while also co-culturing endothelial cells (luminal side) and astrocytes (abluminal side) instead of only using endothelial cells [15]. This system successfully demonstrated that TEER values under flow–based co-culture condition showed 10–fold increase compared to static co-culture. Yet, due to the inside chamber size (2×5 mm^2), the platform still had limitations in the degree of shear stress that could be applied (max 0.0008 dyn/cm^2 applied), which is significantly lower than the condition in brain microcapillaries *in vivo* (5–25 dyn/cm^2) [16–18]. Another similar BBB chip reduced the channel width to 500 μm and increased the shear stress applied to about 5.8 dyn/cm^2, which resulted in increased TEER on this BBB chip [19]. Nevertheless, there still remains a large gap in physiological cellular interactions achieved by these *in vitro* systems compared to the *in vivo* environment. This is partially due to the use of cell lines instead of primary cells. To overcome these potential limitations, another BBB chip by Brown et al. used mostly primary cells, such as primary human endothelial cells, primary human pericytes, and neuronal cells derived from human induced pluripotent stem cells (hiPSCs), although the astrocytes used were cell lines [20]. Thus the system incorporating all the cell types involved in the BBB formation and structure. However, this platform still has the same limitation of significantly lower shear stress applied (0.02 dyn/cm^2) because of their relatively larger chamber size ($3 \times 6.2 \times 1$ mm^3) as with the previous *in vitro* BBB models, limiting the degree of shear stress that can be applied [12]. Here, we present a multi-compartment microfluidic BBB chip that recapitulates the critical functional astrocyte–capillary interface of the BBB, while also allowing up to 16 different assays to be conducted in parallel using each of the 16 BBB units on a single chip. Each of the BBB compartment is equipped with integrated electrical impedance sensors that can measure the permeability of the barrier function continuously and non–invasively. Our approach provides for the first time an *in vitro* BBB chip that satisfies most of the features needed to form an *in vivo*-like BBB chip that is also amenable for medium-throughput screening, namely: (i) controllable and reproducible formation of a realistic brain–capillary interface through co-culture of primary astrocytes and primary brain microvascular endothelial cells on each side of a porous membrane, (ii) optimized choice of extracellular matrix (ECM) that significantly increased the tight junction, (iii) an optimized *in vivo* level shear stress applied to the culture for increased tight junction, (iv) a versatile multi-channel screening architecture that utilizes 4 rows of microfluidic channels that represents the brain side and 4 columns of microfluidic channels that represents the brain capillary side to create 16 semi-independent BBB compartments at their cross–sections, and (vi) integrated electrical impedancesensor array that can non–invasively measure barrier permeability in each of the BBB compartments in real time, continuously, and in parallel.

II. Materials and Methods

A. Microfluidic multi–channel BBB chip design

The microfluidic multi-channel BBB chip is composed of two intersecting poly(dimethylsiloxane) (PDMS) microfluidic channel arrays, a luminal channel array filled with endothelial cell culture media and an abluminal channel array filled with astrocyte cell culture media, placed on each side of a 10 μm thick porous polycarbonate membrane (Fig. 1A). The area where these two microchannels intersect forms a single BBB unit, as

illustrated in Fig. 1B, resulting in a total of 16 semi-independent BBB units on a single chip. This configuration allows the intersecting channels to be connected through the porous membrane, which functions as a physical isolation barrier that separates the two cell types while still allowing diffusion of molecules through the membrane pores. Thus neurovascular endothelial cells and astrocytes, grown in each of the two separate microenvironments, are still connected through the porous membrane to have localized interactions, especially between astrocyte endfeet and endothelial cells. The four top fluidic channels and four bottom fluidic channels combined together allow 16 different conditions to be tested in one experimental run through the multi–channel structure (4 × 4 intersecting channels) (Fig. 1C–E). However, as each channel fluidically connects four BBB units, the 16 units are not completely independent. The four units that are connected through the same channel can be used as technical replicates but not as biological replicates, while the units in a different channel can represent one biological replicate. Each BBB unit in the chip has their own top and bottom electrodes to measure TEER for tight junction analysis, allowing all 16 BBB units to be monitored simultaneously throughout the culture. The TEER electrodes are designed so that microscopic observation of both sides of the channels are still possible during the cell culture (Fig. 1D).

B. Chip fabrication

The BBB chip was fabricated by standard photolithography and assembling techniques. The multi-electrode arrays (MEAs) were fabricated by first depositing a thin titanium adhesion layer (20 nm) and a gold layer (200 nm) on polycarbonate substrates and patterned using standard photolithography and metal etching. The MEAs were designed to have 4 × 4 array electrodes (Fig.1A). The exposed area of each electrode site was 1 cm^2. The MEA-patterned polycarbonate substrates were then cut and the inlet/outlet holes and screw holes made by a laser machining tool (PLS6, Universal Laser Systems, AZ). PDMS (10:1 mixture) prepolymer was spin-coated onto a Si wafer to form a 300 μm thick layer, and then cured for 4 hours at 65 °C. The cured PDMS layer was cut by the laser to make the microfluidic channel array (W, L, H: 1 mm, 19 mm, 300 μm). The cut PDMS layers were attached onto the MEA-patterned substrates and then released. After stamping each PDMS channel layer bonded on the MEA-patterned substrate onto a thin layer of PDMS prepolymer, a 0.4 μm pore polycarbonate membrane (Corning, NY) was placed between these two layers still having uncured thin PDMS prepolymer layers. The two PDMS channel layers on the MEA-patterned substrate were placed perpendicularly to each other. The entire assembly was then placed between two thick poly(methyl methacrylate) (PMMA) substrates (4 mm), and the four screws that are holding the two PMMA substrates together were uniformly tightened to the same level using a gauged torque wrench. The device was then cured in an oven for 4 hours at 65 °C to allow the prepolymer between the channels to cure with the porous membrane for liquid-tight sealing. After loosening the four screws to take out the top PMMA substrate, a PDMS gasket was placed between the top PMMA substrate and the top MEA-patterned substrate to ensure tight sealing between the two layers. Again, the four screws were uniformly tightened using a gauged torque wrench to ensure tight sealing. After autoclaving, the screws were further tightened using the same torque wrench and the inlet/outlet tubings inserted into the top PMMA substrate and then fixed with acryl glue.

C. Primary cell preparation

Primary astrocytes were obtained as previously described [21]. In brief, brains were separated from the forebrains of 1–2 day old C57BL/6 mice. Cortices were dissected under a stereomicroscope and put in ice–cold HBSS (Ca^{2+}/Mg^{2+}-free Hank's Balanced Salt Solution, Invitrogen, CA). Tissues were digested with 0.25% trypsin (Sigma–Aldrich, MO) and DNase (Thermo Fisher Scientific, MA) for 15 min at 37 °C. After digestion, cortices were dissociated by triturating repeatedly using a 10 ml pipette until they became homogenous cells. Dissociated glial cultures were grown in poly–D–lysine coated culture flasks in 10% FBS supplemented DMEM (Thermo Fisher Scientific, MA) containing 1.0 mM Pyruvic acid (P2256, Sigma-Aldrich, MO) and 4.0 mM GlutaMAX (Invitrogen, CA). Astrocytes were purified from the glial layer in the flask that has been exposed to the specific microglia toxin L-leucine methyl ester (1 mM) for 1 h, followed by 1–2 cycles of subculture and repeated exposure to L-leucine methyl ester. Purified astrocytes were maintained in growth medium for 3 days before use. Primary mouse brain microvascular endothelial cells derived from C57BL/6 mice were passaged as previously described [22]. The primary endothelial cells were maintained in 10% FBS supplemented with IMDM (Thermo Fisher Scientific, MA) containing 2.0 mM GlutaMAX (Invitrogen, CA). All animal procedures were approved by the Institutional Animal Care and Use Committee (IACUC) at Texas A&M University (Protocol #2014–0252).

D. Microfluidic perfusion culture in the BBB chip

For astrocyte and endothelial cell co-culture, primary astrocytes were first seeded at a density of 300 cells/mm^2 on ECM-coated BBB chips. Either fibronectin (10 μg/ml, Trevigen, MD) or 10% matrigel (BD Biosciences, CA) was used as the ECM material. Astrocyte culture was maintained in a static culture condition initially to allow the astrocytes to adhere on the microchannels of the chip. After 24 hours from cell seeding, astrocytes continued to be cultured in fresh growth media with extremely low flow rate (0.1 μl/min) provided by a syringe pump (Chemyx, TX) for 6 days. To seed endothelial cells, the chip was flipped over to make the bottom part of the chip the upper side. Primary endothelial cells were seeded at a density of 150 cells/mm^2 on the backside channels of the chip, which were also coated with the same ECM as the astrocyte side. The endothelial cell culture was maintained in static condition first to allow the cells to adhere on the channels of the chip. During this time, the astrocyte culture was also in static condition without any media flow. After 24 hours from seeding endothelial cells, endothelial cells continued to be cultured to proliferate at a growth media flow rate of 1.5 μL/min for 3 days. The shear stress value on the bottom wall (τ_{wall}) of a microfluidic channel was derived from the Navier–Stokes equation describing the fluidic motion inside a rectangular-shaped channel (Equation 1),

$$\tau_{wall} = \frac{6Q\mu}{wh^2} \quad (1)$$

where τ_{wall} is the shear stress, Q is the volumetric flow rate, μ is the dynamic fluid viscosity, w and h indicate the width and height of the channel, respectively. In the case of the

monoculture experiment, only primary endothelial cells were cultured on one side of the BBB chip following the above endothelial cell culture procedure. All cell cultures were maintained at 37 °C in a humidified 5% CO2 incubator.

E. Immunocytochemistry

Cells were fixed in 4% paraformaldehyde for 20 min at 25 °C and permeabilized with 1% Triton X-100 for 10 min at room temperature. After being treated in 5% goat-serum for 1 hour at room temperature, samples were agitated overnight at 4 °C in primary antibodies: anti–zonula occludens-1 (ZO-1, mouse monoclonal, 1:100, Life Technologies, NY) and anti-GFAP (glial fibrillary acidic protein, rabbit, 1:1000, Sigma-Aldrich, MO). Samples were then agitated in secondary antibodies of Alexa 594 goat antimouse (1:1000, Life Technologies, NY) and Alexa 488 goat anti-rabbit (1:1000, Life Technologies, NY) for 1 hour at room temperature. Samples were rinsed with PBS after each step. ZO-1 was used for identification of tight junction proteins among endothelial cells. Positive GFAP labeling identified astrocytes. Nuclei and actin were respectively stained with Hoechst 33342 (1 mg/ml, Life Technologies, NY) and Alexa 594 phalloidin (1:40, Life Technologies, NY) to observe cell morphology on the porous membrane. Fluorescently labeled cells were imaged using an inverted microscope (Olympus, Japan).

F. TEER measurement for non–invasive permeability assessment

To quantitatively assess the barrier permeability non-invasively, TEER was measured using an alternating current (AC) square wave at a frequency of 12.5 Hz using the EVOM2 epithelial volt/ohm meter (WPI, FL). To allow TEER measurements from all 16 BBB units on the chip continuously, a system consisting of a multiplexer (PXI–2530, National Instruments, TX) and a data acquisition board (DMM–4065 (National Instruments, TX) was used. Each of the 16 pairs of TEER measurement electrodes was connected to the multiplexer, which was then connected to the EVOM2 instrument. A LabView™ (National Instruments, TX) program controlled the multiplexer to switch the four wires used by the EVOM2 in a 4 × 16 configuration to each of the electrical contact pads of the electrode array in each of the BBB compartments. The analog TEER values from the EVOM2 were sent to the data acquisition board and graphically displayed on the monitor while recording the values (Fig. 1F).

G. Permeability assessment using fluorescent tracer molecule

In another method for barrier permeability assessment, fluorescent tracer molecules having different molecular sizes were used. A mixture of red-fluorescent dextran 3,000Da (Texas Red dextran, Life Technologies, NY), blue-fluorescent dextran 10,000Da (Alexa 546 dextran, Life Technologies, NY), and green-fluorescent dextran 70,000Da (FITC dextran, Sigma-Aldrich, MO), each at a concentration of 500 μg/ml in culture media, was loaded into the luminal channel of the BBB chip so that dextran could diffuse through the barrier and into the abluminal channel of the chip. After 6 hours in no flow condition, samples were collected from the abluminal channel and the fluorescent intensities measured using a multi–channel fluorescence plate reader (Cytation 5, BioTek Instruments, VT). Fick’s laws of diffusion was used to calculate the permeability coefficient (ratio between the original

dextran concentration and the diffused dextran concentration). All permeability assays were conducted at days *in vitro* (DIV) 4 of endothelial culture.

H. Pharmacological treatments

To confirm that the tight junction barrier formed can be disrupted by pharmacological treatments, 100 μM histamine (EMD Millipore, Germany) in culture media was applied at DIV 4 while continuously measuring the TEER value to monitor the change in barrier permeability in real time.

III. Results and Discussion

A. Growth of primary neurovascular endothelial cells and formation of tight junction in the microfluidic BBB chip

Although the use of cell lines are convenient, endothelial cell lines have shown critical differences in their ability to respond to cytokines and in various functional markers as compared to primary endothelial cells [23, 24]. In this study, primary neurovascular endothelial cells were used in the microfluidic BBB chip. Primary neurovascular endothelial cells grew and proliferated in the device without any observable cell death. The number of endothelial cells growing on the porous membrane area increased gradually and were confluent by DIV 3 as evaluated by actin filament and nuclei staining, respectively (Fig. 2A). Interestingly, a higher cell density was observed inside the porous membrane area not smeared by the PDMS prepolymer during the assembly process and thus exposed to the backside microfluidic channel, as compared to the vicinity of the exposed area of the membrane (Fig. 2B). This significant endothelial cell coverage may improve BBB formation by minimizing endothelial cell loss over the porous membrane area, as in transwell culture the net loss of cells during culture commonly resulted in lower levels of TEER [6].

To investigate whether the primary neurovascular endothelial cells cultured in the microdevice form proper tight junctions, cells were immunostained with an antibody against tight junction protein ZO-1. Fig. 2C shows that as the number of endothelial cells increases from DIV 1 to DIV 4, the expression of ZO-1 also simultaneously increases, indicating the time-dependent formation of tight junctions among the endothelial cells. Importantly, a sharp increase in tight junction formations is observed between DIV 2 and DIV 3. By DIV 4, tight junctions were densely formed throughout the endothelial cell culture, covering the entire area of the exposed porous membrane. Fig. 2D shows an enlarged view of the tight junction formation among endothelial cells.

B. Optimizing BBB chip configuration

B.1. Extracellular matrix (ECM) selection—The basement membrane plays a critical role in cellular interaction and regulation of cell behaviors. The ECM can form an interstitial basement membrane that provides the framework for cell attachment, and thus a reliable ECM is required for *in vitro* BBB models. To investigate how different ECMs affect the degree of tight junction formation, the effects of fibronectin and Matrigel (composed of a mixture of ECM proteins laminin, collagen IV, nidogen/enactin and proteoglycan) on the formation of tight junction were compared by coating each ECM on the porous membrane

in the BBB chip. As shown in Fig. 3, in the case of the fibronectin–coated device, the TEER values increased considerably by 2.5 times over the course of 4 days, from 663 ± 162 Ω at DIV 0 to 1674 ± 427 Ω at DIV 4 (n = 10, p< 0.05), consistent with the time-dependent increases in ZO-1 expression. Similarly, the TEER values in the Matrigel-coated device also increased considerably by 5.5 times, from 615 ± 122 Ω at DIV 0 to 3368 ± 441 Ω at DIV 4 (n = 12, p< 0.001). Importantly, the Matrigel-coated device showed a significantly higher TEER value (2.0 times higher) than that of the fibronectin-coated device (p< 0.05). This finding shows that the use of Matrigel as the basement membrane results in tighter barrier formation with high TEER value, and is thus used throughout the subsequent experiments.

B.2. Optimization of shear stress level—Shear stress plays an important role in cell culture, and although shear stress was applied in previously developed BBB chips, the levels of shear stress applied (0.0008 – 0.15 dyn/cm^2) were significantly lower compared to *in vivo* level shear stress (5 – 25 dyn/cm^2) [15–18, 25]. We hypothesized that applying a shear stress similar to *in vivo* shear stress range may lead to higher degree of tight junction formation. Fig. 4 shows the degree of ZO-1 expression in endothelial cells cultured under 8 different shear stress conditions (0, 1, 5, 10, 15, 20, 25 and 30 dyn/cm^2) applied in the BBB chip by adjusting the luminal side of the culture media flow rate. Compared to the static culture case, ZO-1 expression showed a significant increase when shear stress ranges from 1 to 25 dyn/cm^2 were applied. Shear stress levels of 20 dyn/cm^2 and 25 dyn/cm^2 showed the highest degree of ZO-1 expression (n = 16). On the other hand, when too high of a shear stress was applied (30 dyn/cm^2), ZO-1 expression level actually decreased. Thus, for all subsequent experiments, the optimized shear stress level of 20 dyn/cm^2 was used.

B.3. Astrocyte–endothelial interactions through co-culture—Astrocytes promote BBB formation as well as neurovascular endothelial cell maturation, contributing to tighter junction formation [26]. The main reason is because various molecules that astrocytes produce can induce aspects of BBB phenotypes in endothelial cells, such as the glial–derived neurotrophic factor (GDNF), basic fibroblast growth factor (bFGF), transforming growth factor–β (TGF–β),and angiopoietin 1 (ANG1) acting on the TIE2 endothelium–specific receptor tyrosine kinase2. In addition, astrocytes can affect the expression and polarized localization of P–glycoprotein (a gatekeeper) and GLUT1 (transport barrier) as well as enzyme modulation of γ–glutamyl transpeptidase (γ–GTP) (metabolic barrier).

To investigate the effect of astrocytes on the BBB properties, primary mouse astrocytes were co-cultured with primary endothelial cells in the BBB chip. Following the *in vivo* structure of the neurovascular unit (Fig. 5A), endothelial cells were cultured on the top side and astrocytes on the back side of a porous membrane in the microfluidic BBB chip. Immunocytochemistry images show that astrocytes were properly cultured on the porous membrane, with the endothelial cells cultured on the opposite side of the porous membrane, leading to cellular interactions through the 10 μm thick porous membrane (Fig. 5B). To examine the effect of astrocyte–endothelial interactions, the barrier permeability between co-culture (astrocyte + endothelial cell) and monoculture (endothelial cell only) were compared by using two methods, TEER analysis and dextran permeability assay. As shown in Fig 5C, the permeabilities of both cases were selective according to the Stokes

size of dextran having different molecular sizes (3kDa, 10kDa, and 70kDa). Dextran with smaller Stokes size showed higher permeability as expected, demonstrating that smaller compounds can pass through the barrier easier. The difference between the co-culture condition and the monoculture condition was greatest with the smallest molecule (3kDa dextran), where co-culture with astrocytes showed 2.48 times lower permeability coefficient compared to that of the monoculture case ($n = 8$). This permeability result demonstrates that the microfluidic BBB chip developed here enables size–dependent molecular transport from the luminal channels to the abluminal channels through the established tight junctions. More importantly, the lower permeability of 3kDa dextran in the co-culture condition quantitatively showed that astrocyte interactions with endothelial cells led to tighter barrier formation.

C. Real–time drug response of the BBB chip

To further test the proper functioning of the BBB chip as well as demonstrate the drug testing capability of the chip, histamine treatment to the BBB chip was conducted. Histamine is known to increase endothelial permeability by disrupting the tight junction barriers [26, 27]. TEER values were monitored in real time while 100 μM of histamine was applied to both the monoculture (endothelial cell only) BBB chip and the co-culture (astrocyte + endothelial cell) BBB chip. After culturing endothelial cells for 4 days, real–time TEER recording was conducted to investigate the change in BBB permeability upon histamine treatment. Fig. 6A shows TEER values in the monoculture condition from DIV 0 to DIV 4, which increased from around 0.5 kΩ to around 2.5 kΩ. In the astrocyte co-culture condition, the TEER values increased from around 0.6 kΩ and then saturated around 3.6 – 4.5 kΩ (Fig. 6B). When 100 μM histamine–containing media was injected only into the luminal channel where endothelial cells reside, an immediate decrease in TEER value was observed in the monoculture condition (Fig. 6C), where it decreased to around 0.5 kΩ (81% lower than the DIV 4 TEER value) within 4 hours. The TEER value then showed a slow recovery over time, eventually saturating to about 1.6 kΩ (62% of the DIV 4 TEER level) in about 4 hours (Fig. 6C). On the other hand, astrocyte co-culture condition did not show any drastic decrease in the TEER value under 100 μM histamine treatment (Fig. 6D). Initially, the average TEER value of the co-culture condition was higher than that of the monoculture condition (2.77 ± 0.32 kΩ vs. 4.48 ± 0.79 kΩ, $n \geq 12$) (Fig. 6E). Comparing the two cases during histamine treatment (Fig. 6F), it is clear that the BBB formed through astrocyte-endothelial cell co-culture (106.37 ± 2.80%, $n = 12$) showed much higher resilient in its barrier function compared to the monoculture case (51.67 ± 9.97%, $n = 4$). As can be seen in Fig. 6E, TEER value before histamine treatment showed a much higher value in the co-culture compared to the case of mono-culture, as also indicated in Fig. 5C where the barrier permeability for the co-culture case was significantly lower as measured through the dextran permeability assay. However, in the case of co-culture, the TEER value did not drop even after histamine treatment, contrary to the case for mono-culture. This stable BBB permeability with co-culture against histamine treatment could be related to the role of astrocytes in regulating histamine clearance or inactivation to avoid histaminergic neuronal activity by plasma membrane monoamine transporter (PMAT), organic cation transporter 3 (OCT3), and histamine N–methyltransferase (HNMT) [28–30].

D. Future applications

Based on the robust multi-channel microfluidic BBB chip demonstrated here and full characterization of its barrier function and multi-modal permeability assays, the next step will be to conduct a pilot-scale drug screening assay using the multi-channel structure. We anticipate that a single chip having 16 semi-independent BBB compartments as shown here can be utilized to test drug compounds at 4 different concentrations, each with 4 replicates, where each permeability can be measured in 4 different locations of one synchronized blood vessel. Conducting such drug testing with compounds with known *in vivo* data and comparing the *in vitro* data to the available *in vivo* mice data will be a major milestone in the development of the BBB-on-a-chip, and more broadly to the organ-on-a-chip community. We have used primary mouse cells in this work, essentially establishing a rodent-on-a-chip, as the generated *in vitro* data can be compared to the wealth of available rodent *in vivo* data, which makes it ideal for *in vitro* to *in vivo* comparison. Comparing animal *in vitro* data to human *in vivo* data would be another major milestone, as *in vivo* animal models are most commonly used to test the toxicity of potential therapeutic candidates, but rodent results have predicted only 43% of human toxicity [31]. This indicates that animal studies are limited in predicting human toxicity despite the high cost of such testing [32]. In this regard, another future step of our *in vitro* BBB system is to test the system with all primary human cells to understand whether human organ–on–a–chip systems can indeed successfully predict drug efficacy and toxicity before clinical trials.

IV. Conclusion

A microfluidic multi-channel BBB chip model with integrated electrical impedance sensor array for label-free barrier function analysis has been successfully developed. The developed system includes features that closely mimic the *in vivo* structures of the BBB and a multitude of physiological functions, including i) more effective selection of ECM, ii) optimized *in vivo* level shear stress applied, and iii) using primary neurovascular endothelial cells co-cultured with primary astrocytes, all contributing to increased level of tight junction formation. The barrier function was confirmed using three different methods, immunofluorescent staining, TEER measurement, and fluorescent molecular permeability assay. The system also provided preliminary evidence of a more realistic drug response of brain tissue protection when exposed to histamine treatment, as is the case in *in vivo* BBB. The 16 BBB units on a single chip can also open up the possibility of medium-throughput drug screening. In these regards, the developed *in vitro* BBB system has the potential to replace or minimize the use of animal studies by effectively predicting the BBB permeability against various drug candidates that are in preclinical stages.

Acknowledgments

This work was partially funded by the National Institutes of Health (NIH) Grant #1R21EB021005-01.

References

[1]. Esch EW, Bahinski A, and Huh D, “Organs-on-chips at the frontiers of drug discovery,” Nat Rev Drug Discov, vol. 14, no. 4, pp. 248–260, 04//print, 2015. [PubMed: 25792263]

[2]. Pangalos MN, Schechter LE, and Hurko O, “Drug development for CNS disorders: strategies for balancing risk and reducing attrition,” Nat Rev Drug Discov, vol. 6, no. 7, pp. 521–532, 07//print, 2007. [PubMed: 17599084]

[3]. Stamatovic SM, Keep RF, and Andjelkovic AV, “Brain Endothelial Cell-Cell Junctions: How to “Open” the Blood Brain Barrier,” Current Neuropharmacology, vol. 6, no. 3, pp. 179–192, 2008. [PubMed: 19506719]

[4]. Loscher W, and Potschka H, “Drug resistance in brain diseases and the role of drug efflux transporters,” Nat Rev Neurosci, vol. 6, no. 8, pp. 591–602, Aug, 2005. [PubMed: 16025095]

[5]. Berezowski V, Landry C, Lundquist S, Dehouck L, Cecchelli R, Dehouck MP, and Fenart L, “Transport screening of drug cocktails through an in vitro blood-brain barrier: is it a good strategy for increasing the throughput of the discovery pipeline?,” Pharm Res, vol. 21, no. 5, pp. 756–60, May, 2004. [PubMed: 15180330]

[6]. Palmiotti CA, Prasad S, Naik, Abul KM, Sajja RK, Achyuta AH, and Cucullo L, “In vitro cerebrovascular modeling in the 21st century: current and prospective technologies,” Pharm Res, vol. 31, no. 12, pp. 3229–50, Dec, 2014. [PubMed: 25098812]

[7]. Cucullo L, Hossain M, Puvenna V, Marchi N, and Janigro D, “The role of shear stress in Blood-Brain Barrier endothelial physiology,” BMC neuroscience, vol. 12, no. 1, pp. 40, 2011. [PubMed: 21569296]

[8]. Colgan OC, Ferguson G, Collins NT, Murphy RP, Meade G, Cahill PA, and Cummins PM, “Regulation of bovine brain microvascular endothelial tight junction assembly and barrier function by laminar shear stress,” Am J Physiol Heart Circ Physiol, vol. 292, no. 6, pp. H3190–7, Jun, 2007. [PubMed: 17308001]

[9]. Santaguida S, Janigro D, Hossain M, Oby E, Rapp E, and Cucullo L, “Side by side comparison between dynamic versus static models of blood–brain barrier in vitro: a permeability study,” Brain research, vol. 1109, no. 1, pp. 1–13, 2006. [PubMed: 16857178]

[10]. Cucullo L, McAllister MS, Kight K, Krizanac-Bengez L, Marroni M, Mayberg MR, Stanness KA, and Janigro D, “A new dynamic in vitro model for the multidimensional study of astrocyte–endothelial cell interactions at the blood–brain barrier,” Brain Research, vol. 951, no. 2, pp. 243–254, 10/4/, 2002. [PubMed: 12270503]

[11]. Cucullo L, Hossain M, Tierney W, and Janigro D, “A new dynamic in vitro modular capillaries-venules modular system: Cerebrovascular physiology in a box,” BMC Neuroscience, vol. 14, no. 1, pp. 18, 2013. [PubMed: 23388041]

[12]. van der Helm MW, van der Meer AD, Eijkel JCT, van den Berg A, and Segerink LI, “Microfluidic organ-on-chip technology for blood-brain barrier research,” Tissue Barriers, vol. 4, no. 1, pp. e1142493, 2016/01/02, 2016. [PubMed: 27141422]

[13]. Prabhakarpandian B, Shen M-C, Nichols JB, Mills IR, Sidoryk-Wegrzynowicz M, Aschner M, and Pant K, “SyM-BBB: a microfluidic blood brain barrier model,” Lab on a Chip, vol. 13, no. 6, pp. 1093–1101, 2013. [PubMed: 23344641]

[14]. Achyuta AKH, Conway AJ, Crouse RB, Bannister EC, Lee RN, Katnik CP, Behensky AA, Cuevas J, and Sundaram SS, “A modular approach to create a neurovascular unit-on-a-chip,” Lab on a Chip, vol. 13, no. 4, pp. 542–553, 2013. [PubMed: 23108480]

[15]. Booth R, and Kim H, “Characterization of a microfluidic in vitro model of the blood-brain barrier (muBBB),” Lab Chip, vol. 12, no. 10, pp. 1784–92, Apr 24, 2012. [PubMed: 22422217]

[16]. Koutsiaris AG, Tachmitzi SV, Batis N, Kotoula MG, Karabatsas CH, Tsironi E, and Chatzoulis DZ, “Volume flow and wall shear stress quantification in the human conjunctival capillaries and post-capillary venules in vivo,” Biorheology, vol. 44, no. 5–6, pp. 375–86, 2007. [PubMed: 18401076]

[17]. Desai SY, Marroni M, Cucullo L, Krizanac-Bengez L, Mayberg MR, Hossain MT, Grant GG, and Janigro D, “Mechanisms of endothelial survival under shear stress,” Endothelium, vol. 9, no. 2, pp. 89–102, 2002. [PubMed: 12200960]

[18]. Cucullo L, Marchi N, Hossain M, and Janigro D, “A dynamic in vitro BBB model for the study of immune cell trafficking into the central nervous system,” J Cereb Blood Flow Metab, vol. 31, no. 2, pp. 767–77, Feb, 2011. [PubMed: 20842162]

[19]. Griep L, Wolbers F, De Wagenaar B, Ter Braak P, Weksler B, Romero IA, Couraud P, Vermes I, Van der Meer A, and Van den Berg A, "BBB on chip: microfluidic platform to mechanically and biochemically modulate blood-brain barrier function," Biomedical microdevices, vol. 15, no. 1, pp. 145–150, 2013. [PubMed: 22955726]

[20]. Brown JA, Pensabene V, Markov DA, Allwardt V, Neely MD, Shi M, Britt CM, Hoilett OS, Yang Q, Brewer BM, Samson PC, McCawley LJ, May JM, Webb DJ, Li D, Bowman AB, Reiserer RS, and Wikswo JP, "Recreating blood-brain barrier physiology and structure on chip: A novel neurovascular microfluidic bioreactor," Biomicrofluidics, vol. 9, no. 5, pp. 054124, 2015. [PubMed: 26576206]

[21]. Kim S, Steelman AJ, Koito H, and Li J, "Astrocytes promote TNF-mediated toxicity to oligodendrocyte precursors," J Neurochem, vol. 116, no. 1, pp. 53–66, Jan, 2011. [PubMed: 21044081]

[22]. Sapatino BV, Welsh CJ, Smith CA, Bebo BF, and Linthicum DS, "Cloned mouse cerebrovascular endothelial cells that maintain their differentiation markers for factor VIII, low density lipoprotein, and angiotensin-converting enzyme," In Vitro Cell Dev Biol Anim, vol. 29A, no. 12, pp. 923–8, Dec, 1993. [PubMed: 8167915]

[23]. Pan C, Kumar C, Bohl S, Klingmueller U, and Mann M, "Comparative proteomic phenotyping of cell lines and primary cells to assess preservation of cell type-specific functions," Mol Cell Proteomics, vol. 8, no. 3, pp. 443–50, Mar, 2009. [PubMed: 18952599]

[24]. Lidington EA, Moyes DL, McCormack AM, and Rose ML, "A comparison of primary endothelial cells and endothelial cell lines for studies of immune interactions," Transpl Immunol, vol. 7, no. 4, pp. 239–46, Dec, 1999. [PubMed: 10638837]

[25]. Walter FR, Valkai S, Kincses A, Petneházi A, Czeller T, Veszelka S, Ormos P, Deli MA, and Dér A, "A versatile lab-on-a-chip tool for modeling biological barriers," Sensors and Actuators B: Chemical, vol. 222, pp. 1209–1219, 1//, 2016.

[26]. Abbott NJ, Ronnback L, and Hansson E, "Astrocyte-endothelial interactions at the blood-brain barrier," Nat Rev Neurosci, vol. 7, no. 1, pp. 41–53, 01//print, 2006. [PubMed: 16371949]

[27]. Dejana E, "Endothelial cell-cell junctions: happy together," Nat Rev Mol Cell Biol, vol. 5, no. 4, pp. 261–270, 04//print, 2004. [PubMed: 15071551]

[28]. Yoshikawa T, Naganuma F, Iida T, Nakamura T, Harada R, Mohsen AS, Kasajima A, Sasano H, and Yanai K, "Molecular mechanism of histamine clearance by primary human astrocytes," Glia, vol. 61, no. 6, pp. 905–16, Jun, 2013. [PubMed: 23505051]

[29]. Schwartz JC, Arrang JM, Garbarg M, Pollard H, and Ruat M, "Histaminergic transmission in the mammalian brain," Physiol Rev, vol. 71, no. 1, pp. 1–51, Jan, 1991. [PubMed: 1846044]

[30]. Perdan-Pirkmajer K, Pirkmajer S, Raztresen A, and Krzan M, "Regional characteristics of histamine uptake into neonatal rat astrocytes," Neurochem Res, vol. 38, no. 7, pp. 1348–59, Jul, 2013. [PubMed: 23549734]

[31]. Olson H, Betton G, Robinson D, Thomas K, Monro A, Kolaja G, Lilly P, Sanders J, Sipes G, Bracken W, Dorato M, Van Deun K, Smith P, Berger B, and Heller A, "Concordance of the toxicity of pharmaceuticals in humans and in animals," Regul Toxicol Pharmacol, vol. 32, no. 1, pp. 56–67, Aug, 2000. [PubMed: 11029269]

[32]. Fielden MR, and Kolaja KL, "The role of early in vivo toxicity testing in drug discovery toxicology," Expert Opin Drug Saf, vol. 7, no. 2, pp. 107–10, Mar, 2008. [PubMed: 18324874]

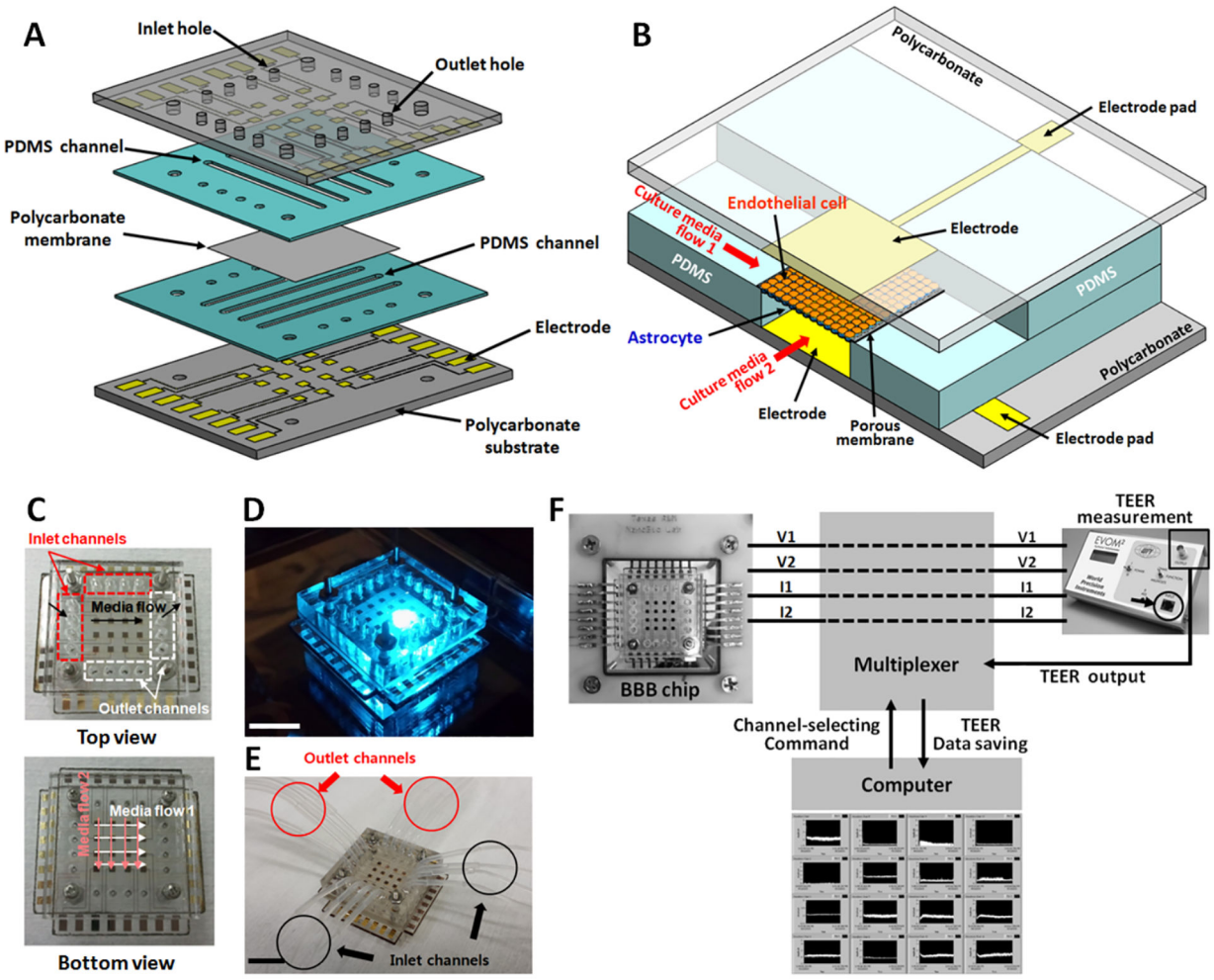

Fig. 1.

The developed multi-channel multi-layer BBB chip with integrated electrical impedance sensor array for TEER analysis. (A) 3D illustration showing the multi-layer structure. (B) 3D structure of a single BBB unit of the 16-unit BBB chip. (C) Intersecting PDMS microfluidic channel arrays, the luminal channel array (for endothelial cell culture) and the abluminal channel array (for astrocyte culture). (D) Photograph of an assembled device on an inverted fluorescent microscope. (E) A fabricated microfluidic BBB chip connected with inlet and outlet tubings and ready for testing. (F) Real–time multi-site TEER recording setup. The BBB chip is connected to an epithelial volt/ohmmeter through a multiplexer. A Labview program is used to monitor the TEER value from all 16 sites. (Scale bar: 10 mm)

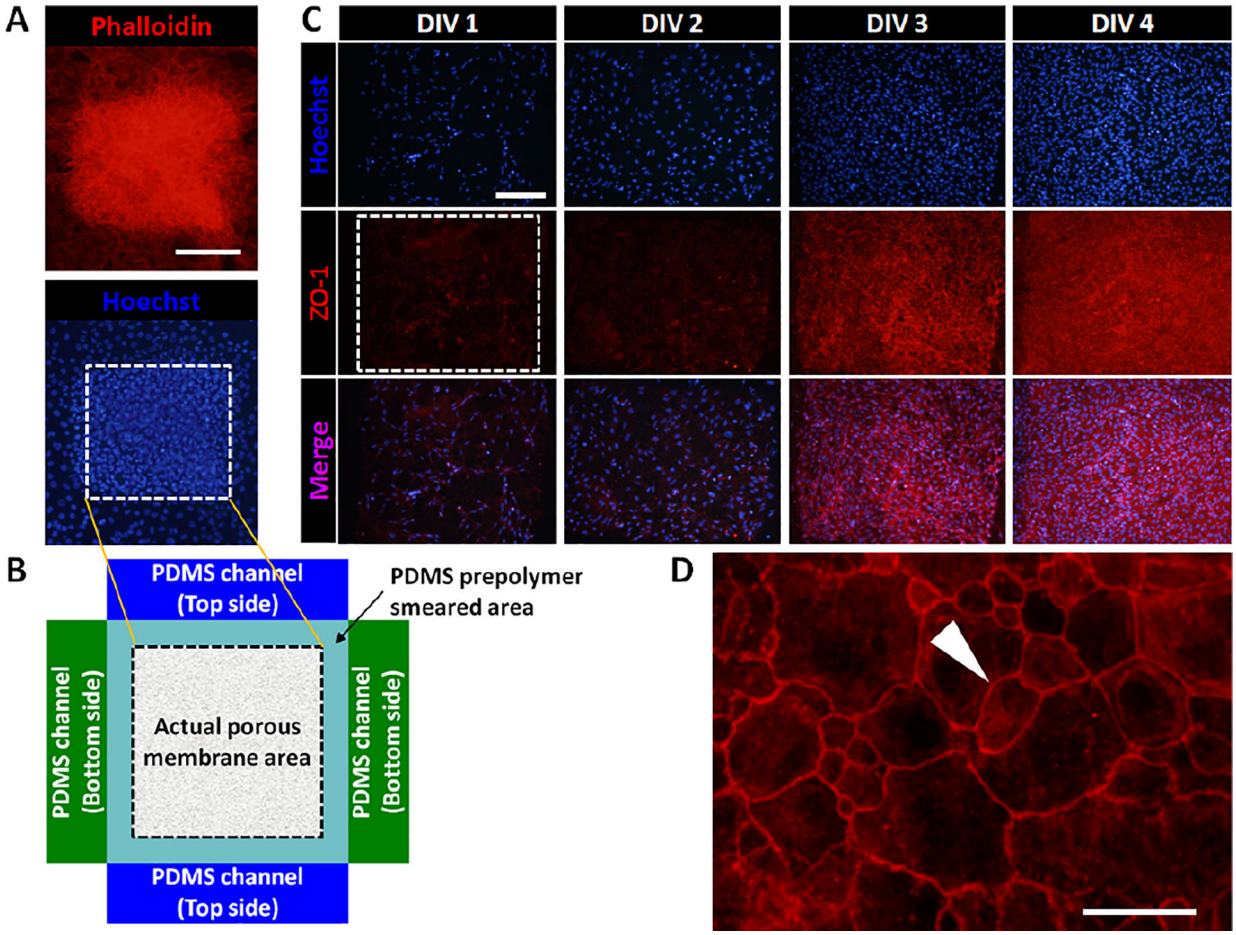

Fig. 2.

(A) Fluorescent images showing primary neurovascular endothelial cells (C57BL/6) cultured on top of the porous membrane in the BBB chip (red: phalloidin stain for actin, blue: hoechst stain for nuclei). Dotted box indicates the area of the exposed porous membrane. (B) A drawing showing the actual exposed area of the porous membrane not smeared by PDMS prepolymer during the chip assembly process. (C) Immunocytochemistry showing endothelial cell growth and formation of tight junctions using tight junction protein ZO-1 (blue: hoechst stain for nuclei, red: ZO-1 stain for tight junction). Scale bars: 200 μm. (D) Enlarged ZO-1 image showing tight junctions. Arrowhead indicates tight junctions. Scale bar: 50 μm.

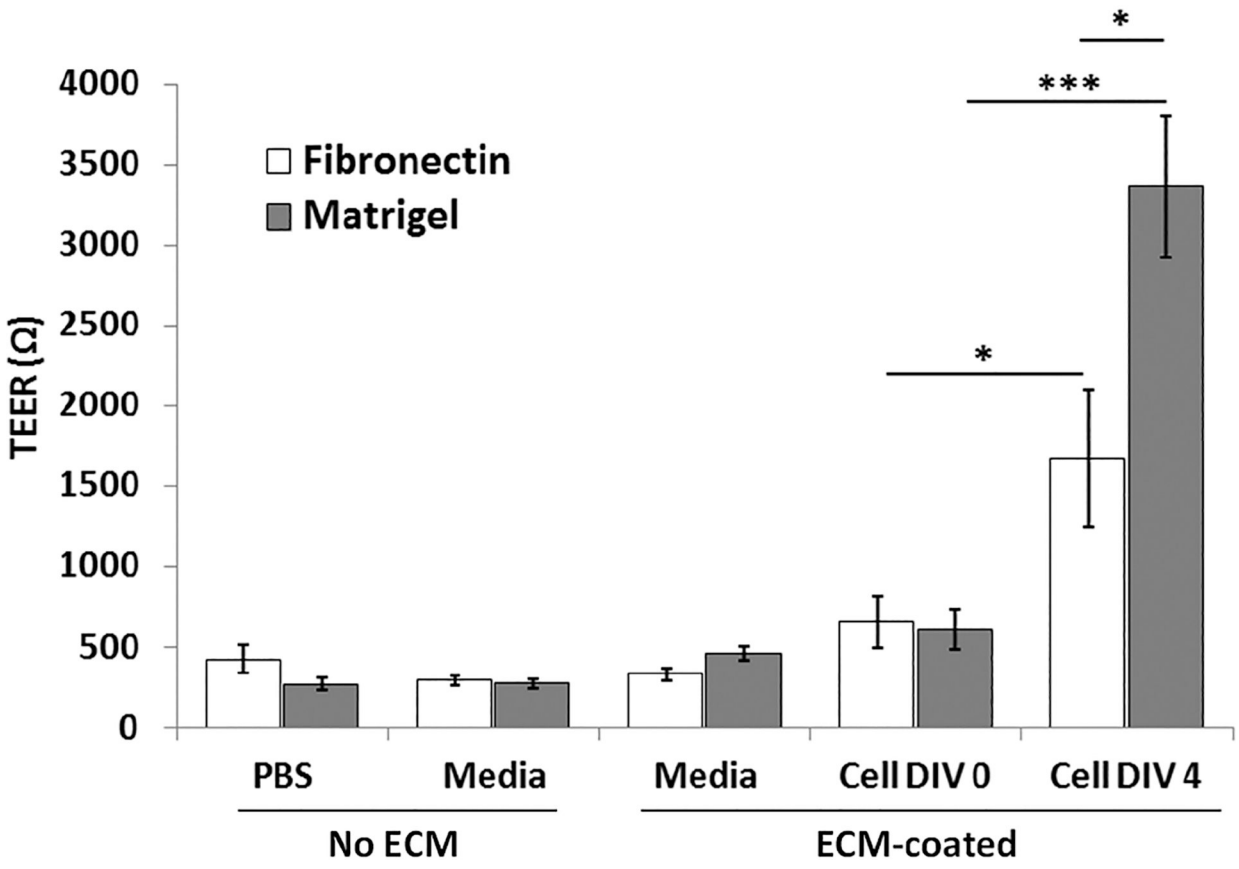

Fig. 3.

Effect of fibronectin and Matrigel coating of the porous membrane on tight junction formation. PBS, media, and media ECM-coated have no cells loaded in the device. TEER measurements were taken 12 hour after cell seeding (DIV 0), and then again after 4 days (DIV 4). All values are plotted as mean ± standard error of the mean. * $p < 0.05$, *** $p < 0.001$.

A

In vivo shear stress level

Shear stress τ_{wall} (dyne/cm²)	Flow rate Q (µL/min)
0	Static
1	0.075
5	0.375
10	0.750
15	1.125
20	1.500
25	1.875
30	2.250

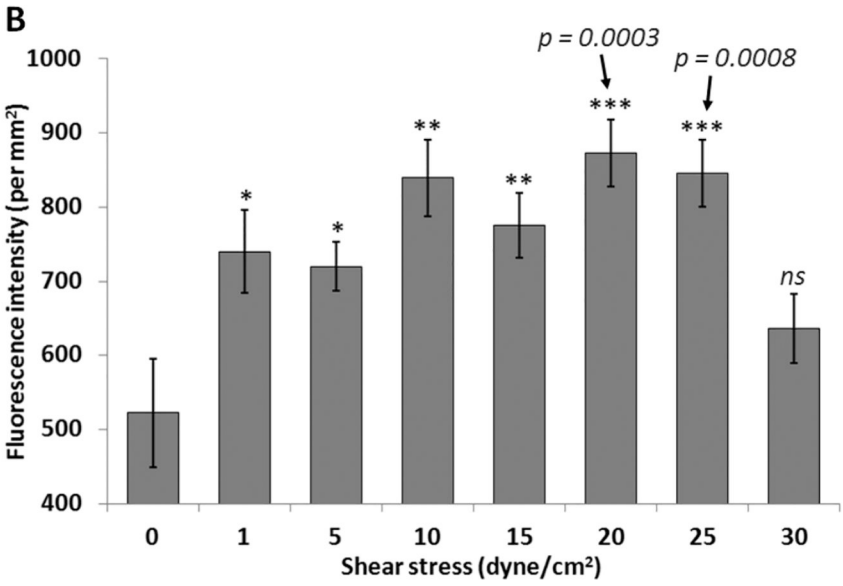

Fig. 4.

The effect of shear stress on tight junction. (A) Culture media flow rates (Q, µl/min) corresponding to the various shear stress (τ_{wall}, dyn/cm^2) tested. Gray highlights indicate *in vivo* level shear stress in the brain blood vessels. (B) Fluorescent intensity per mm^2 displaying ZO-1 expression in endothelial cells inside the BBB chip (static culture for 1 day, followed by perfusion culture for 3 days). All values are plotted as mean ± standard error of the mean (n = 16). * p< 0.05, ** p< 0.01, *** p< 0.001.

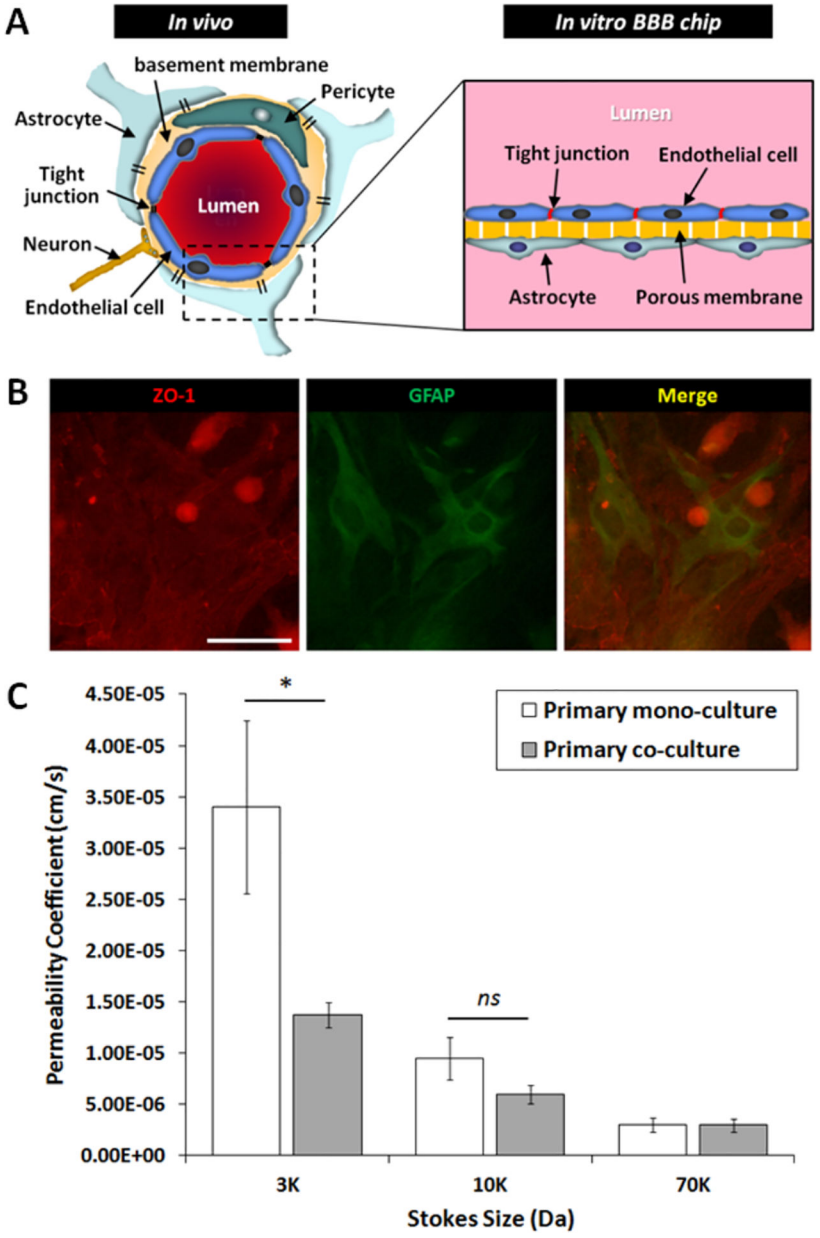

Fig. 5.

Effect of astrocyte–endothelial co-culture on barrier permeability. (A) Schematic cross section of an *in vivo* neurovascular unit compared to the structure of the *in vitro* BBB chip developed here. (B) Immunocytochemistry images of astrocyte-endothelial cell co-culture on the same porous membrane interface (endothelial cells on the front side and astrocytes on the back side) of the BBB chip. Tight junction: ZO-1 staining (red), astrocyte: GFAP staining (green). Scale bar: 100 μm. (C) Fluorescent dextran permeability depending on dextran sizes. Only the smallest dextran size (3kDa) showed a significant difference between monoculture and co-culture ($p = 0.0168$). All values are plotted as mean ± standard error of the mean. * $p < 0.05$, *ns* (no significant difference).

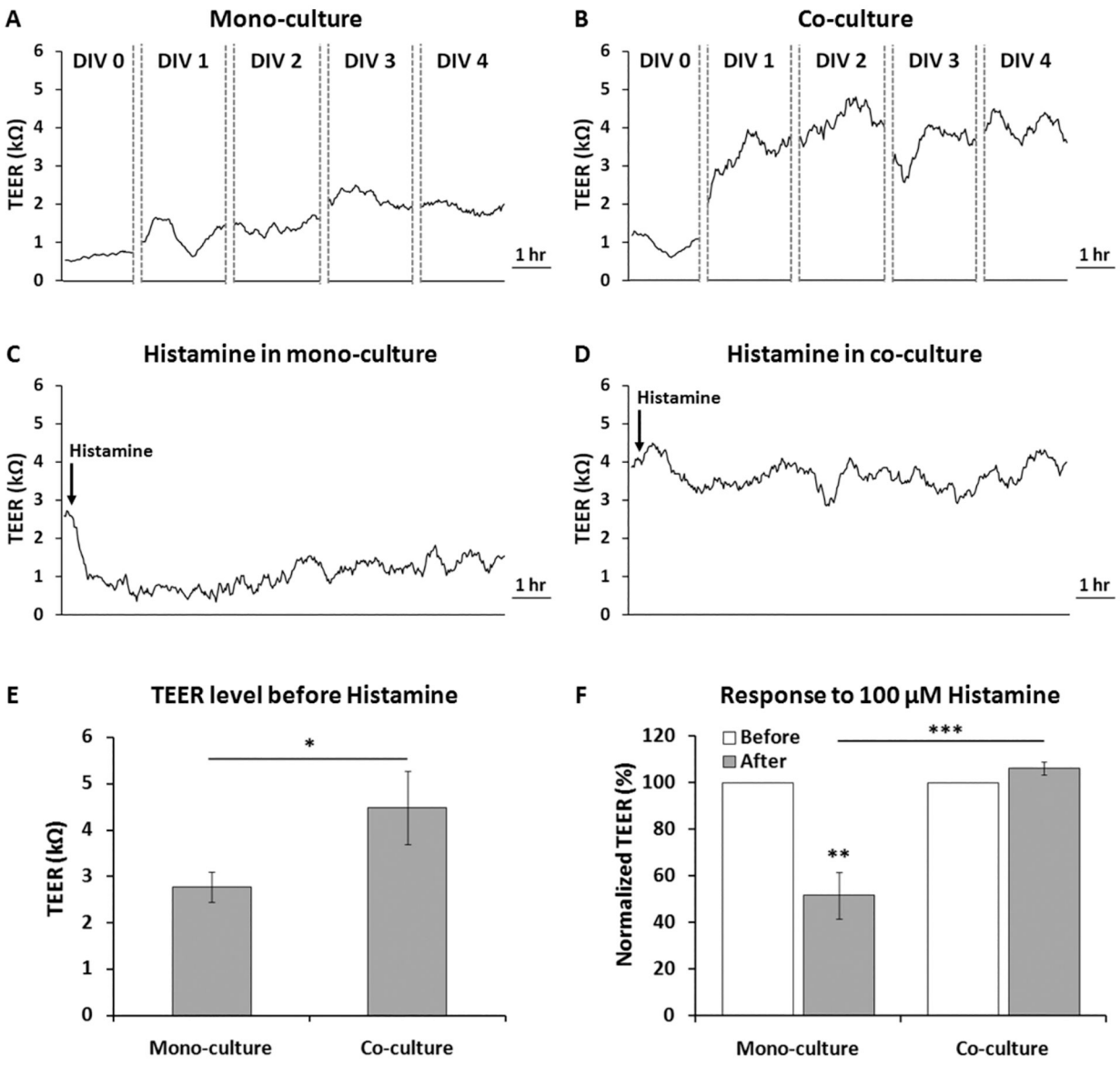

Fig. 6.

Real–time TEER measurement in the BBB chip during drug treatment. (A) TEER values during monoculture (endothelial cell only, DIV 0 – DIV 4). (B) TEER values during co-culture (endothelial cell and astrocyte, DIV 0 – DIV 4). (C) TEER values in response to100 µM histamine treatment in the monoculture case. (D) TEER values in response to 100 µM histamine treatment in the co-culture case. (E) Comparing TEER values from monoculture vs. co-culture at DIV 4. (F) Percentage changes in normalized TEER ($TEER_{after}$ / $TEER_{before}$ × 100) after 100 µM histamine treatment. * $p< 0.05$, ** $p< 0.01$, *** $p< 0.001$.